Poll Res. 39 (2) : 278-282 (2020)

ISSN 0257–8050

ADSORPTION KINETICS AND ISOTHERM STUDY ON PHOSPHATE REMOVAL FROM AQUEOUS SOLUTION BY *SAPINDUS EMARGINATUS*

P. MERCY JASPER AND S. SUMITHRA*

Department of Environmental Sciences, Yogi Vemana University, Kadapa, Andhra Pradesh, India.

(Received 26 September, 2019; accepted 26 December, 2019)

ABSTRACT

Phosphate pollution is a major concern for soil and water management. In the present study *Sapindus emarginatus* seed powder was used to remove phosphate. The parameters such as initial concentration, contact time, dosage, pH and temperature were optimized. All experiments were done at room temperature except temperature studies. The Langmuir adsorption capacity of *Sapindus emarginatus* was found to be 6.765 mg/g. The kinetic data of phosphate adsorption was fitted well with the pseudo second order model. With the increase in temperature the phosphate removal was decreased.

KEY WORDS : Phosphate, Adsorption, *Sapindus emarginatus*, Temperature.

INTRODUCTION

The high level of phosphate entering in the water bodies could cause eutrophication, which stimulates algal population and aquatic plants and continues to be a global issue (Wan *et al.,* 2017) and surface water bodies around the globe, for instance, lakes, reservoirs, lagoons, rivers, streams, and estuaries are facing the risk of eutrophication (Ashekuzzaman and Jiang, 2014). The phosphate when applied as fertilizer to agricultural soil, the crop will take little amount and the remaining is being lost to the environment via surface runoff and drainage (Saadat *et al.,* 2018a). There are various techniques available for the removal of phosphate among that adsorption has been an alternative due to their environmental friendliness, simple operation and highly efficient, non-toxic, and has a wide range of phosphate concentration, therefore used to remove phosphate from water (Goscianska *et al.,* 2018). Some of the adsorbents that have been used to remove phosphate include rice husk (Gawande *et al.,* 2017), thermally modified copper tailings (Zhou *et al.,* 2019) chitosan (Jung *et al.,* 2015a), eggshell ash (Torit and Phihusut, 2018), magnesium slag particles (Tang *et al.,* 2017), sludge derived biochar (Saadat *et al.,* 2018b), core shell material (Si *et al.,* 2018). The objective of the present work is to investigate the efficiency of removal of phosphate from aqueous solution by *Sapindus emarginatus*.

MATERIALS AND METHODS

In order to prepare stock solution, 1.4329 g of anhydrous potassium dihydrogen phosphate (KH_2PO_4) was dissolved in 1000 mL of distilled water. This stock solution was stored in a brown colored glass bottle and diluted to prepare required concentration. The natural solution pH 6.9 was kept constant during the experiment. *Sapindus emarginatus* seeds were brought from local market. The seeds are washed with normal water two times and then washed with distilled water one time. After washing the seeds is dried in hot air oven at 60 ^{o}C. Seeds were grounded and sieved with 25 microns and were used as biosorbent.

Adsorption experiment

The batch adsorption studies were done in 250 mL conical flask filled with 50 mL of adsorbate at different initial concentration 20 – 60 mg/L, quantity dose of 400 mg was added into the solution and

agitated at 180 rpm in a rotary shaker. The final concentration of phosphate was measured in double beam UV- visible spectrophotometer (Lab India UV 3000+) at a wave length of 690 nm. The phosphate removal and equilibrium adsorption uptake, q_e (mg/g) was calculated using the following relationships.

$$\text{Percent removal} = 100 \frac{(C_o - C_e)}{C_o} \quad .. (1)$$

$$\text{Amount adsorbed } (q_e) = \frac{(C_o - C_e)\, V}{w} \quad .. (2)$$

Where C_o is the initial adsorbate concentration (mg/L), C_e is the equilibrium adsorbate concentration (mg/L), V is the volume of the solution (L) and w is the mass of the adsorbent.

RESULTS AND DISCUSSION

Impact of contact time and initial concentration

The amount of phosphate adsorption increased from 20 to 60 mg/L of the initial phosphate concentration provided an important driving force for the phosphate to overcome the mass transfer resistance between adsorbent and solution (Almasi *et al.*, 2012). The initial adsorption rate was relatively rapid and then attains equilibrium. The amount of phosphate adsorption at equilibrium increased from 2.3 to 5.5 mg/g with increase in phosphate concentrations (Fig. 1). This is in accord to the results of phosphorus removal by eggshell ash (Torit and Phihusut, 2018).

Adsorption kinetics of *Sapindus emarginatus* seed

Phosphate adsorption kinetics was interpreted with Lagergren first order, pseudo second order and Elovich model. Table 1 lists the calculated kinetic parameter values. The pseudo-second-order kinetic model fit well with the data when compared to other kinetic models indicating that chemical bonding between adsorbent active sites and phosphate might dominate the adsorption process (Fig. 2). This model showed the highest R^2 (0.9882) value and the calculated q_e (3.127 mg/g) were close to the experimental q_e (3.157) for 30 mg/L. Our findings are similar to the adsorption of phosphate onto CaO-biochar composites (Liu *et al.*, 2019), by sludge derived biochar (Saadat *et al.*, 2018b).

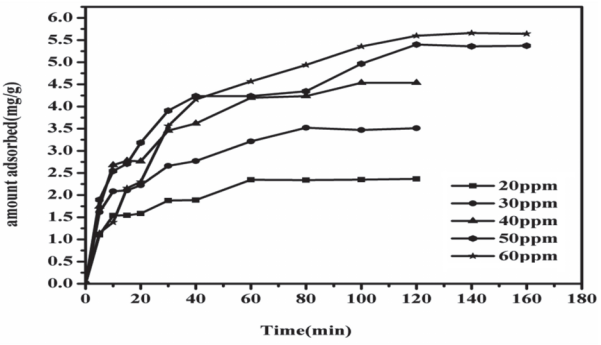

Fig. 1. Effect of contact time on phosphate adsorption

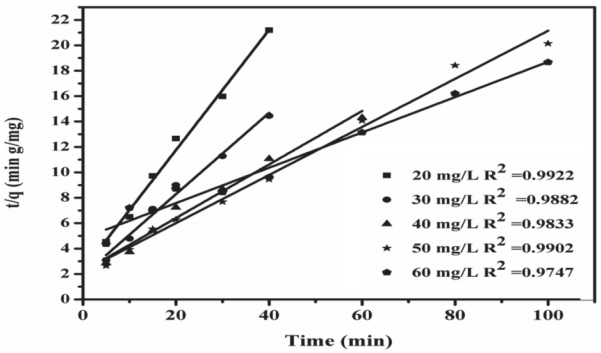

Fig. 2. Second order kinetics plot for the removal of phosphate

Table 1. Kinetic model sustained values for seed of *Sapindus emarginatus* – phosphate adsorption.

Model	Kinetic parameters	Initial phosphate concentration (mg/L)				
		20	30	40	50	60
Pseudo first –order	$q_e$exp(mg/g)	2.348	3.157	4.236	5.398	5.599
	K_1(min^{-1})	-0.027	-0.039	-0.068	-0.018	-0.029
	$q_e$cal (mg/g)	1.232	1.802	4.453	3.283	5.367
	R^2	0.8859	0.9633	0.8831	0.9046	0.9812
Pseudo second -order	$q_e$cal (mg/g)	2.114	3.127	4.748	5.282	7.194
	K_2(min^{-1})	0.097	0.064	0.020	0.016	0.004
	R^2	0.9922	0.9882	0.9833	0.9902	0.9743
Elovich	α	1.081	1.653	1.336	1.820	0.471
	β	2.283	1.682	1.114	0.951	0.643
	R^2	0.9154	0.9563	0.9639	0.9636	0.9694

Adsorption Isotherms of phosphate on *Sapindus emarginatus* seed

Experimental data were applied to linear and non – linear forms of Langmuir, Freundlich and Dubinin – Radushkevich (D-R) isotherms (Fig. 3 and Table 2). Q_o is the mono layer adsorption capacity (mg/g), b is the Langmuir affinity coefficient related to the energy of adsorption (L/mg). The linear form of the Freundlich isotherm model fitted well, suggesting that heterogeneous layer of phosphate adsorption occurred onto the surface of *Sapindus emarginatus*. The Langmuir adsorption capacity of phosphate onto *Sapindus emarginatus* was found to be 6.76 mg/g. The adsorption capacity of montmorillonite was observed to be 0.228 mg/g (Fang *et al.,* 2017), iron oxide tailings reported as 1.29 mg/g (Sima *et al.,* 2018) and peanut shell derived biochar were found to be 6.79 mg/g (Jung *et al.,* 2015b) respectively.

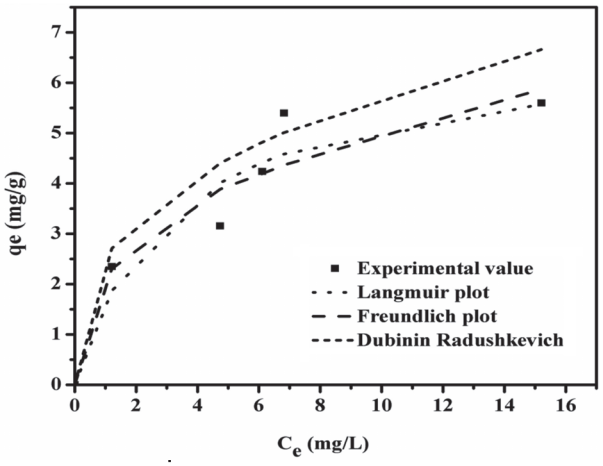

Fig. 3. Adsorption isotherms of phosphate

The effect of solution pH and desorption studies

Concentrations of ions are considered as one of the vital parameters that influence the adsorption of ions. The maximum phosphate removal was recorded at pH 5.0 to be 80 % for 50 mg/L (Fig. 4). Lower adsorption is observed at high pH values because there is a competition for the adsorption sites between phosphate species and OH– ions. In addition at high pH values there is repulsion of negatively charged PO_4^{3-} species. Similar phenomenon was also reported in the adsorption of phosphate onto peat based biosorbents (Robalds *et al.,* 2016).

Desorption studies shows that regeneration of spent adsorbent and recovery of the phosphate would make the treatment process economical. Incomplete desorption of phosphate at different concentration confirmed that the chemisorptions

Table 2. Isotherm parameters for adsorption of phosphate

Langmuir constants			
C_o (mg/L)	Q_o (mg/g)	b (L/mg)	R_L
20	6.765	0.307	0.140
30			0.097
40			0.075
50			0.061
60			0.051
Freundlich constants			
C_o (mg/L)	k_f ($mg^{1-1/n}\ L^{1/n}\ g^{-1}$)	n	R^2
20	2.149	2.707	0.8463
30			
40			
50			
60			
Dubinin-Radushkevich constants			
C_o (mg/L)	q_m (mg/g)	E (kJ/mol)	R^2
20			
30	148.180	26.730	0.8462
40			
50			
60			

Table 3. Thermodynamic parameters for the adsorption of phosphate

Temperature (°C)	K_c	ΔG^o (KJ/mol)	ΔH^o (KJ/mol)	ΔS^o (J/mol/K)
32	1.9372	-1.6766	101.391	- 326.611
40	0.7837	0.634		
50	0.2093	4.2005		

was the major mode of adsorption.

Thermodynamic parameters

Thermodynamic parameters for the adsorption of phosphate on to seed powder of *Sapindus emarginatus* was calculated by the following equation and are presented in Table 3.

$$\Delta G^o = -RT \ln K_c \quad .. (3)$$

Where R is gas constant (8.314 J/mol/K), b is equilibrium constant (L/mol) and T is the temperature in (K):

$$\log K_c = (\Delta S^o/2.303 \times R) - (\Delta H^o/ 2.303 \times RT) \quad .. (4)$$

The values of ΔH^o and ΔS^o were determined from the slope and intercept of Van't Hoff plots log K_c vs 1/T. Positive values of ΔH^o suggest the endothermic nature of adsorption. The negative and positive values of ΔG^o indicate spontaneous nature of adsorption and involved strong chemical reaction. The negative value of ΔS^o with *Sapindus emarginatus* indicate decreased randomness at the solid solution interface.

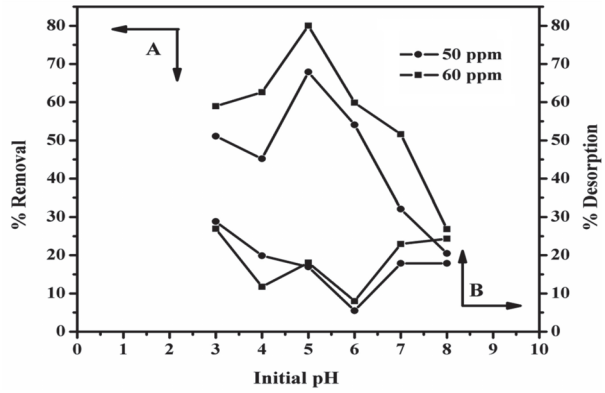

Fig. 4. Effect of pH on adsorption and desorption of phosphate

Characterization of *Sapindus emarginatus*

The physical and chemical components of the adsorbent have been presented in Table 4. The specific gravity and porosity was observed as 1.25 and 29 .04 %. The SEM micrograph presented in the Fig. 5. showed the surface texture and porosity of *Sapindus emarginatus* before and after adsorption. The FTIR spectra of the *Sapindus emarginatus* before and after adsorption are shown in Fig 6. Appearance of broad band around 3421 cm^{-1} indicates the presence of both free and hydrogen bonded – OH

Table 4. Characteristics of the adsorbent

1	pH zpc	3.7
2.	Bulk Density (g/mL)	0.887
3	Mechanical Moisture Content (%)	4.3
4.	Ash Content (%)	6.26
5.	pH	5.67
6.	EC (µs/cm)	0.69
7.	Water soluble Content (%)	11.07
8.	Acid Soluble Content (%)	19.85
9.	Sodium (Na) (ppm)	147.2
10.	Potassium (K) (ppm)	141.4
11.	Calcium (Ca) (ppm)	Not detected
12.	Phosphate (ppm)	8
13.	Decolorizing power (mg/g)	120
14.	Specific gravity	1.25
15.	Porosity (%)	29.04

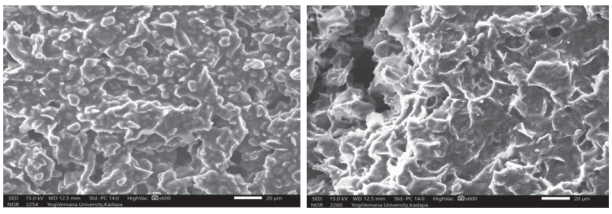

(a) (b)

Fig. 5. SEM images of *Sapindus emarginatus* (a) before adsorption and (b) after adsorption of phosphate.

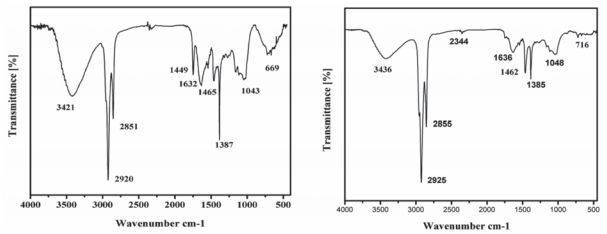

(a) (b)

Fig. 6. FTIR images of (a) unloaded and (b) loaded adsorbent.

groups onto the adsorbent surface. It is also found that there are shift in the peaks from 669 cm^{-1} to 716 cm^{-1} in the unloaded and loaded adsorbent and appearance of new bands in the loaded adsorbent at 2344 cm^{-1}. The peaks around 1632 cm^{-1} correspond to C=C stretching (Bui *et al.,* 2018).

CONCLUSION

In this work *Sapindus emarginatus* was used as adsorbent to remove phosphate in aqueous solution. The adsorption kinetics data followed pseudo – second order kinetic model. The equilibrium adsorption data obeyed Freundlich isotherm. Increase in adsorbent dosage increased the percentage removal of phosphate. Maximum removal of phosphate was observed at pH 5.0. The positive values of ΔH^o indicate the endothermic nature of adsorption. This result suggests that *Sapindus emarginatus* can be effectively used to adsorb phosphate from aqueous solution.

REFERENCES

Almasi, A., Omidi, M., Khodadadian, M., Khamutian, R. and Gholivand, M.B. 2012.Lead (II) and cadmium (II) removal from aqueous solution using processed walnut shell: kinetic and equilibrium study. *Toxicological and Environmental Chemistry.* 94: 660-671.

Ashekuzzaman, S. and Jiang, J. Q. 2014. Study on the sorption-desorption-regeneration performance of Ca-, Mg- and CaMg based layered double hydroxides for removing phosphate from water. *Chemical Engineering Journal.* 246 : 97-105.

Bui, T., Hong, S. P. and Yoon, J. 2018. Development of nanoscale zirconium molybdate embedded anion exchange resin for selective removal of phosphate *Water Research.* 134 : 22-31.

Fang, H. W., Cui, Z. H., He, C. J., Huang, L. and Chen, M.H. 2017. Phosphorus adsorption onto clay minerals and iron oxide with consideration of heterogeneous particle morphology. *Sci. Total Environ.* 605 : 357-367.

Gawande, S. M., Shelke, P.K., Dhoke, N.A., Lengre, M. D. and Dere, D.A. 2017. Analysis and removal of phosphate from wastewater by using rice husk. *International Research J. of Eng. and Techol.* 4: 2115- 2119.

Goscianska, J., Ptaszkowska - Koniarz, M., Frankowski, M. and Franus, M. 2018. Panek R., Franus W. Removal of phosphate from water by lanthanum-modified zeolites obtained from fly ash. *J. of Colloid and Interface Science.* 513 : 72-81.

Jung, K. W., Hwang, M. J., Ahn, K. H. and Ok, Y. S. 2015b. Kinetic study on phosphate removal from aqueous solution by biochar derived from peanut shell as renewable adsorptive media. *Int. J. Environ. Sci. Technol.* 12 : 3363-3372.

Jung, K.Y., An, B., Choi, J. W., Park, C. and Lee, S. H. 2015a. Separation of phosphate from wastewater using an ion exchanger based on chitosan. *Global Environmental Research.* 19 : 35-42.

Liu, X., Shen, F. and Qi, X. 2019. Adsorption recovery of phosphate from aqueous solution by CaO-biochar composites prepared from eggshell and rice straw. *Science of the Total Environment.* 666 : 694-702.

Robalds, A., Dreijalte, L., Bikovens, O. and Klavins, M. 2016. A novel peat-based biosorbent for the removal of phosphate from synthetic and real wastewater and possible utilization of spent sorbent in land application. *Desalination and Water Treatment.* 57 : 13285-13294.

Saadat, S., Bowling, L., Frankenberger, J. and Kladivko, E. 2018a. Nitrate and phosphorus transport through subsurface drains under free and controlled drainage. *Water Res.* 142 : 196-207.

Saadat, S., Raei, E. and Talebbeydokhti, N. 2018b. Enhanced removal of phosphate from aqueous solutions using a modified sludge derived biochar: Comparative study of various modifying cations and RSM based optimization of pyrolysis parameters. *J of Environmental Management.* 225 : 75-83.

Si, Q., Zhu, Q. and Xing, Z. 2018. Simultaneous removal of nitrogen and phosphorus by magnesium - modified calcium silicate core - shell material in water. *Ecotoxicology and Environmental Safety.* 168 : 656-664.

Sima, T. V., Letshwenyo, M. W. and Lebogang, L. 2018. Efficiency of waste clinker ash and iron oxide tailings for phosphorus removal from tertiary wastewater: Batch studies. *Environmental Tech. and Innovation.* 11 : 49-63.

Tang, X., Li, R., Wu, M., Dong, L. and Wang, Z. 2017. Enhanced phosphorus removal using acid - treated magnesium slag particles. *Environmental Science and Pollution Research.* 25 : 1-12.

Torit, J. and Phihusut, D. 2018. Phosphorus removal from wastewater using eggshell ash. *Environmental Science and Pollution Research.* 1- 9.

Wan, S., Wang, S., Li, Y. and Gao, B. 2017. Functionalizing biochar with Mg-Al and Mg-Fe layered double hydroxides for removal of phosphate from aqueous solutions. *Journal of Industrial and Engineering Chemistry.* 47 : 246 - 253.

Zhou, R., Wang, Y., Zhang, M., Yu, P.X. and Li, J. 2019. Adsorptive removal of phosphate from aqueous solutions by thermally modified copper tailings. *Environ. Monit. Assess.* 191-198.